Appl. Phys. B 66, 393–396 (1998)

Applied Physics B
Lasers
and Optics
© Springer-Verlag 1998

Rapid communication

Enhancement of the photorefractive effect by homogeneous pyroelectric fields

N. Korneev[1], D. Mayorga[1], S. Stepanov[1], A. Gerwens[2], K. Buse[2], E. Krätzig[2]

[1] INAOE, Apt. Postal 51 y 216, CP 72000, Puebla, Pue., Mexico
[2] Fachbereich Physik, Universität Osnabrück, D-49 069 Osnabrück, Germany

Received: 12 January 1998

Abstract. Spatially uniform heating or cooling of a photorefractive strontium–barium niobate crystal yields large pyroelectric fields. Two-beam coupling measurements and observation of beam intensity profiles behind the crystal reveal that drift of charge carriers in the pyroelectric field strongly enhances the photorefractive effect. Illumination by a continuous wave laser beam causes large pyroelectric fields via absorption and heating. The drift in pyroelectric fields must be taken into account as a transport mechanism if pyroelectric crystals are used. This mechanism is promising for novel photorefractive devices.

PACS: 42.65.Hw; 77.70.+a; 78.20.Jq

In photorefractive crystals inhomogeneous illumination redistributes charge carriers, space charge fields build up and modulate the refractive index via the electro-optic effect. Volume holographic data storage and outstanding wavelength filtering are two examples of promising applications of photorefractive materials [1–3], and the number of new ideas for using the crystals grows rapidly. For the optimization of the materials and for the proper design of photorefractive devices, an understanding of the charge transport processes is required.

Drift, diffusion, and the bulk photovoltaic effect are the charge driving forces [4] that are usually taken into consideration. Pyroelectric fields, which can be created in many photorefractive crystals, make a contribution to the drift current [5]. Thermal gratings formed in a crystal by inhomogeneous illumination and absorption cause the formation of an electric field grating via the pyroelectric effect. Its influence is twofold. On the one hand it modulates the refractive index directly via the electro-optic effect [6] and on the other hand it affects the process of charge transport. Because the distance between bright and dark regions in holographic experiments is only a few μm, heat conductivity smoothes the temperature pattern and the modulated part of the pyroelectric fields is negligible for typical continuous wave laser light intensities ($< 100\,\mathrm{kW\,m^{-2}}$) [7, 8]. However, a strong pyroelectric grating can be created by pulsed lasers. The influence of the inhomogeneous pyroelectric fields on the charge transport was considered, and experiments were performed which revealed that, if laser pulses are utilized, the drift in pyroelectric fields can be the dominant charge driving force [5, 8, 9].

However, in experiments with cw light the crystal is heated homogeneously by the absorbed light power. Then surface polarization charges are formed, which produces an electric field acting in the same way in the region of photorefractive grating formation as a field externally applied to the sample. The influence on beam fanning [10] and on two-wave mixing gain [11] has been studied. But the gratings generated by homogeneous pyroelectric fields are assumed to be of an unshifted type, and thus beam fanning and two–wave mixing are rather indirect ways to investigate this effect.

Here, we report on experiments which reveal that these homogeneous pyroelectric fields can influence the charge transport significantly and that they are of general importance in all pyroelectric photorefractive crystals.

The pyroelectric fields can become rather high. With $E_{\mathrm{pyro}} = (\partial P_{\mathrm{s}}/\partial T)(\varepsilon\varepsilon_0)^{-1}\Delta T$ and $\Delta T = Pt(Mc_{\mathrm{p}})^{-1}$ we find that 100 mW absorbed power creates a field of $E_{\mathrm{pyro}} = 2.5\,\mathrm{kV/cm}$ in a strontium-barium niobate crystal of 1 g (approximately $0.2\,\mathrm{cm}^3$) within 10 s, where $\partial P_{\mathrm{s}}/\partial T$ is the pyroelectric coefficient, ε the dielectric constant, ΔT the change in temperature, P the absorbed power, t the heating time, M the mass, and c_{p} the specific heat capacity. The material parameters used are summarized in [8].

In contrast to the usual experiments with an external field, the pyroelectric field will be compensated by moving charges. Thus the pyroelectrically driven effect will be transient. Let us assume that the crystal is first heated in the dark, so that the pyroelectric field is $E_{\mathrm{pyro},0}$, and subsequently the crystal is illuminated with a sinusoidal interference pattern, illumination starting from the instant $t = 0$. This yields a spatially averaged photoconductivity σ and the homogeneous pyroelectric field will be compensated with a characteristic time equal to the dielectric relaxation time $\tau_{\mathrm{M}} = \varepsilon\varepsilon_0/\sigma$. The field decreases according to $E_{\mathrm{pyro}}(t) = E_{\mathrm{pyro},0}\exp(-t/\tau_{\mathrm{M}})$. If we assume a grating of small spatial frequency, the buildup of the space charge field E_{sc} is described by the differential equation $E_{\mathrm{sc}}(t) + \tau_{\mathrm{M}}\,\mathrm{d}E_{\mathrm{sc}}/\mathrm{d}t = -mE_{\mathrm{pyro}}(t)$, where m is the fringe contrast.

Diffusion and bulk photovoltaic effects can be neglected in our case. The solution for the space charge field is

$$E_{sc}(t) = -mE_{pyro,0}(t/\tau_M)\exp(-t/\tau_M)\,. \quad (1)$$

The field $|E_{sc}(t)|$ starts from zero at $t = 0$, reaches the maximum value $|mE_{pyro,0}/e|$ at $t = \tau_M$, where $e = \exp(1)$, and goes to zero for $t \gg \tau_M$. Thus the amplitude of the space charge field can reach about 1/3 of the pyroelectric field. If heating or cooling occurs during recording, the equations have to be modified. However, if temperature changes are faster than τ_M, the presented theoretical considerations are still valid.

We investigate a cerium-doped strontium–barium niobate crystal ($Sr_xBa_{1-x}Nb_2O_6$) of the congruently melting composition ($x = 0.61$, SBN). Doping with cerium was performed by adding 0.1 wt% CeO_2 to the melt. After the sample has been cut, all sides are polished to optical quality and the crystal is contacted by silver paste electrodes on the surfaces perpendicular to the axis of spontaneous polarization (*c* axis). The sample is polarized by heating to 120 °C and cooling to room temperature with an externally applied electric field of 10 kV/cm. The dimensions of the sample are $a \times b \times c = 5.78\,\text{mm} \times 3.84\,\text{mm} \times 2.98\,\text{mm}$; in all experiments the light propagates along the *b* direction.

Light from a HeNe laser (light wavelength 632.8 nm) is split into two beams which enter the crystal symmetrically. The beam diameters are about 1 mm (full $1/e^2$ width), each beam has a power of 1 mW, and the light is ordinarily polarized. In some experiments the contrast ratio of the interference pattern is reduced by illumination by an additional incoherent HeNe laser beam. The grating vector is aligned parallel to the *c* axis and a small angle of 0.6° between surface normal and the beams is used, which yields a period length of the interference pattern of about 30 μm. We use the standard method for the investigation of unshifted gratings [12]. One of the laser beams is phase-modulated by means of a vibrating mirror with an amplitude of $\Delta\Phi = 1$ rad and a frequency $f = 250$ Hz. A photodiode is placed behind the crystal in another beam. The interaction of beams with the grating produces an ac signal on the photodetector and it is measured with a lock-in amplifier.

The modulation depth m_{time} of the first-harmonic signal is defined as the ratio between the amplitude and the averaged value of the light intensity. To get some information about the magnitude of the pyroelectric currents, the crystal is short-circuited, heated by illumination, and the currents are measured by a voltmeter with an input resistance of 10 MΩ. Furthermore, experiments with extraordinarily polarized HeNe laser light are carried out. We observe the intensity pattern of different beams behind the crystal with a CCD camera.

Electrical and optical heating of the crystal are performed. We place the sample on a glass plate which can be heated by using a resistive device with a power of up to 2 W. Alternatively, the crystal is illuminated by a beam of a frequency-doubled cw Nd:YAG laser (wavelength 532 nm, beam diameter approximately 3 mm) with a power of 100 mW.

Typical experimental results are shown in Figs. 1 and 2. For a constant temperature there is practically no first-harmonic signal on the photodetector (Figs. 1 and 2, part A). Subsequent electrical heating and cooling after the heating is off yields a strong signal (Fig. 1, parts B and C). During

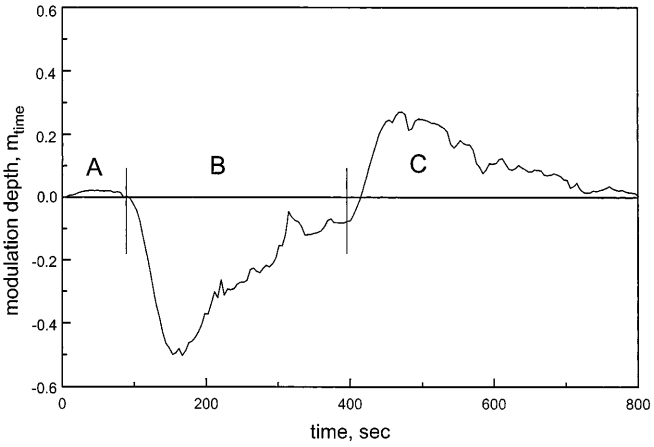

Fig. 1. Modulation depth m_{time} of the light intensity of one of the two interfering beams of a HeNe laser (632.8 nm) behind the crystal versus time *t*. Another recording beam is phase-modulated and the pattern contrast is close to unity. The initial period is A, and during period B the crystal is heated externally with an electrical power of 0.74 W. Then, during C, the heating is switched off and the crystal cools down

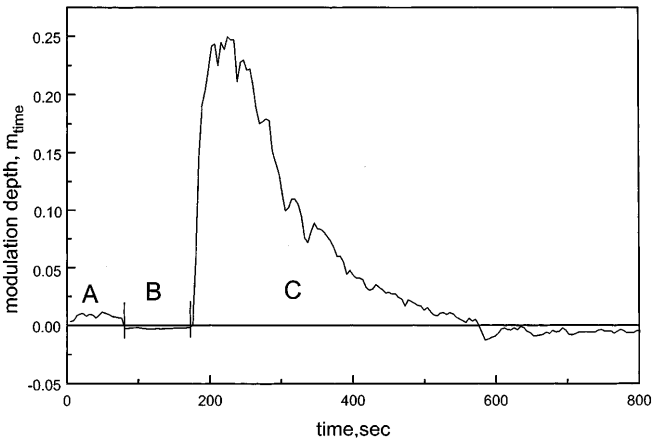

Fig. 2. Modulation depth m_{time} of the light intensity of one of the two interfering beams of a HeNe laser (632.8 nm) behind the crystal versus time *t*. Another recording beam is phase-modulated and the pattern contrast is close to unity. A is the initial period, and during period B the crystal is heated by illumination with a beam of a cw frequency-doubled Nd:YAG laser (light wavelength 532 nm, power 100 mW, full $1/e^2$ diameter 3 mm). Then, during C, the heating is switched off and the crystal cools down

light-induced heating the signal is small (Fig. 2, part B), but after the green light is switched off, the crystal cools down and a strong signal appears (Fig. 2, part C). The sign of the signal is different for cooling and for heating. The maximum of the modulation depth m_{time} shows a linear dependence on the heating power up to 1 W (Fig. 3). In this experiment the interference contrast is reduced to 0.27 by illumination by an additional incoherent laser beam. For larger heating powers there is a risk of depolarizing the crystal. We look also for the second-harmonic signal; it is always small and not influenced by heating or cooling. Direct measurement of the pyroelectric current created in the short-circuited regime by illumination with the 100-mW Nd:YAG laser beam shows an initial peak of (10.5 ± 0.5) nA which decreases exponentially with a time constant of (20 ± 5) s.

Some experiments with extraordinarily polarized light are carried out. In this case the interaction is stronger because

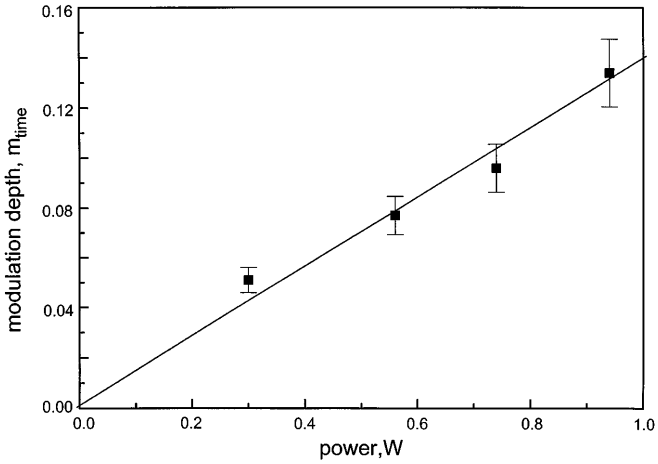

Fig. 3. Maximum of modulation depth $|m_{time}|$ as a function of electrical heating power P. Wavelength and interference contrast of the recording beams are 632.8 nm and 0.27. The symbols are measured data and the solid line is a linear fit

of the higher electro-optic coefficient used, and therefore beams can become distorted. A beam of the HeNe laser ($1/e^2$ diameter about 1 mm) is focused by a cylindrical lens (focal length 20 cm) into the crystal (light stripe perpendicular to the c axis). Figure 4 shows the evolution of the intensity profile of the beam behind the sample. The same heating and cooling cycle as in Fig. 1 is applied. The beam is distorted during temperature changes, but in the steady-state situation the initial pattern is always restored. Illumination by a circular beam focused into the crystal shows asymmetrical defocusing at the beginning, with the formation of regular patterns which are more pronounced in the direction of the c axis. Finally, the beam breaks into a speckle-like pattern. Unfocused beams also break into a speckle pattern for high levels of heating. Figure 5 shows that heating the crystal during interaction of two beams at first yields the appearance of higher diffraction orders and later this pattern becomes distorted. In this experiment the two-wave mixing geometry described above is used, but the angle between the beams is reduced to 0.03°.

All results are well explained considering the charge transport in homogeneous pyroelectric fields. Diffusion will not influence the unshifted part of the grating which is detected by the first-harmonic signal [12]. Furthermore, diffusion is weak because of the large fringe spacing. The SBN:Ce crystals show practically no bulk photovoltaic effect [13], and no external electric fields are applied. Thus the appearance of the large observed signals during heating or cooling is a proof of the presence of homogeneous pyroelectric fields. For heating and cooling, the signs of the pyroelectric fields are different. This yields a switch of the phase position of the grating of π and a change of the sign of the first-harmonic

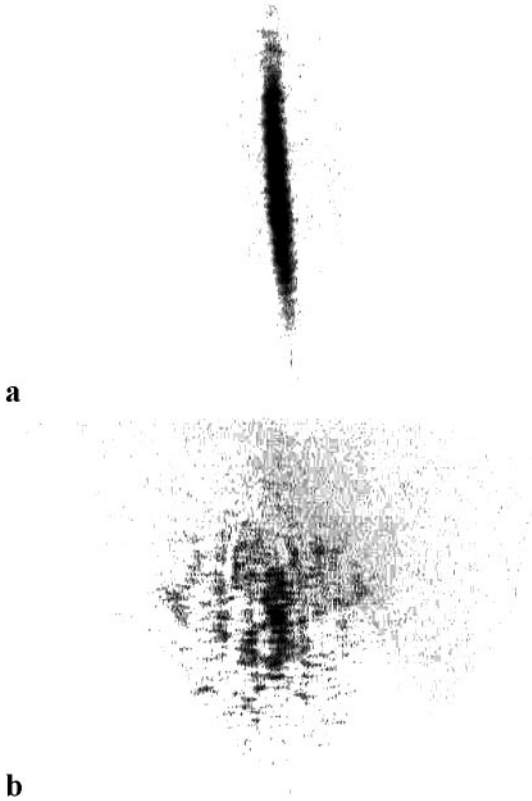

Fig. 4a,b. Images of a beam behind the crystal. An extraordinarily polarized laser beam is focused by a cylindrical lens into the crystal, the rear face of the sample is imaged onto a CCD camera, and the pictures obtained are processed electronically to invert the contrast. The c axis is aligned horizontally and both images have the same scale and contrast. **a** shows the beam profile in the steady-state situation and **b** during heating or cooling when the interaction becomes maximum. The power of the external electrical heating is 1 W

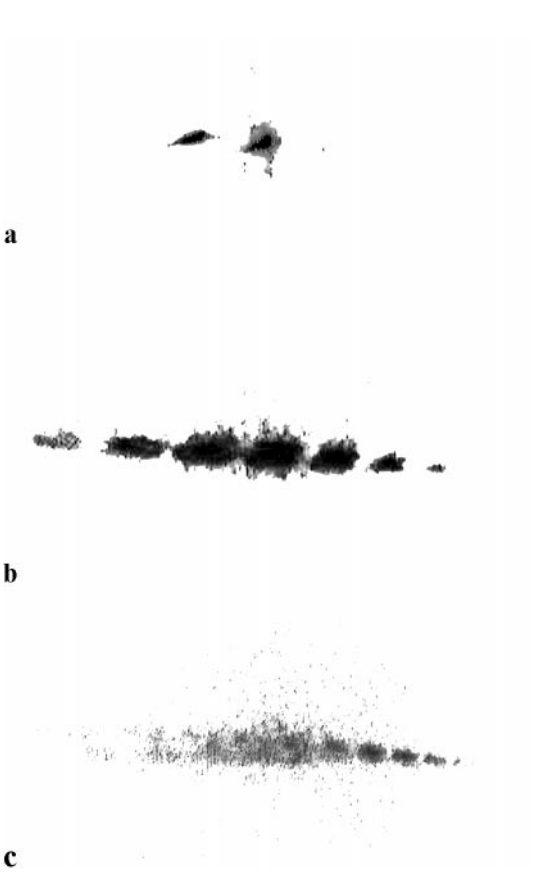

Fig. 5a–c. Far-field images of two interfering beams behind the crystal. The c axis is aligned horizontally and all images have the same scale and contrast. **a** shows the steady-state situation, **b** the pattern during the beginning of heating or cooling, and **c** the intensity profile when the interaction becomes a maximum. The power of the external electrical heating is 1 W

signal when the heating is switched off and the crystal begins to cool down. It is obvious that no signal is observed during light-induced heating (Fig. 2, period B); the green light yields a large conductivity and erases the grating written by the red light. Furthermore, the conductivity induced by the green light short-circuits the pyroelectric fields.

It is known that in the case of an unshifted phase grating the modulation depth m_{time} is given by the following equation [12]

$$m_{\text{time}} = 2\pi\ \Delta\Phi\ \Delta n\, b/\lambda\ , \tag{2}$$

where Δn is the amplitude of the refractive index grating, b the thickness of the crystal and λ the vacuum light wavelength. This equation is valid only for $\Delta\Phi \ll 1$. We use $\Delta\Phi = 1$ and the reduction of the fringe contrast can be considered by the correction factor 0.68. The refractive index change is given by $\Delta n_{\text{o}} = -n_{\text{o}}^3 r_{13} E_{\text{sc}}/2$, where n_{o} is the ordinary refractive index, r_{13} the electro-optic coefficient and E_{sc} the amplitude of the space charge field. By considering $\Delta n \propto E_{\text{sc}}$, the qualitative behavior of the signals (Figs. 1 and 2) is well explained by (1) and (2).

We obtain up to $m_{\text{time}} = 0.5$ (Fig. 1, section B) and (2) yields $\Delta n = 1.9 \times 10^{-5}$. With $n_{\text{o}} = 2.31$ and $r_{13} = 50\,\text{pm/V}$ we get $E_{\text{sc}} = 0.6\,\text{kV/cm}$. Thus, from (1), the homogeneous pyroelectric field is $E_{\text{pyro}} \approx 2\,\text{kV/cm}$. This field is close to the coercive field of SBN, and it is lower than the value estimated from current integration. A more detailed analysis would require consideration of how the fields close to the coercive field influence crystal parameters. Furthermore, depending on the experimental situation, the illuminated crystal region might be clamped by the dark surrounding and then only the primary pyroelectric effect would be present. In SBN the secondary pyroelectric effect is small compared to the primary one [14], but in other materials the secondary effect may be of importance. For extraordinarily polarized light the refractive index changes are larger because $r_{33} \approx 5 \times r_{13}$ [15]. The photographs (Figs. 4 and 5) show impressively that the refractive index changes are large enough to create beam instabilities.

Integration of the directly measured pyroelectric current yields a pyroelectric field of 12 kV/cm. But this does not mean that this field is developed in an open-circuit regime, because the coercive field in SBN is only 2 kV/cm and when the field approaches this value the pyroelectric coefficient is strongly modified. Furthermore, compensation by mobile charges from the crystal or air ions may reduce the fields. For a given heating power and heating time the pyroelectric field is proportional to $(\partial P_{\text{s}}/\partial T)(\varepsilon\rho c_{\text{p}})^{-1}$. With the parameters summarized in [8], we calculate this coefficient for different oxidic ferroelectric crystals and normalize the results to that for SBN. The results are: SBN, 1; $KNbO_3$, 3.4; $BaTiO_3$, 3.0; $KTa_{0.52}Nb_{0.48}O_3$ (KTN), 0.8; $LiNbO_3$, 2.4; and $LiTaO_3$, 4.0. This shows that in all these materials a strong influence of homogeneous pyroelectric fields is possible.

Pyroelectric fields are of general interest and importance for many reasons: (1) Refractive index changes can be enlarged without an external electric field. (2) The fields can influence the processes in many photorefractive devices, for example in volume holographic memories. (3) Beam instabilities caused by these fields may influence phase conjugating mirrors and single beam propagation, for example it is interesting to see whether transient beam instabilities, which play a crucial role in phase conjugators [16], can be attributed to the presented effect. (4) Electrical fixing and frequency doubling in periodically poled material can be influenced by pyroelectric fields. (5) Details of the pyroelectric effect, like the coercive field, can be studied by using an optical technique. (6) Incoherent beams can interact via the absorbed light energy which opens new opportunities for optical switching and processing. (7) Because of heat conductivity, interaction of non-overlapping beams is possible.

In conclusion, electrical or optical heating of ferroelectric photorefractive crystals yields large pyroelectric fields. These fields can influence the charge transport in a similar way to externally applied electric fields, if the crystals are not short-circuited. Even heating with cw beams can create pyroelectric fields which are large enough to play a dominant role in the charge transport processes.

Acknowledgements. Financial support from the Volkswagen-Stiftung (project I/72347) is gratefully acknowledged.

References

1. F.S. Chen, J.T. LaMacchia, D.B. Fraser: Appl. Phys. Lett. **13**, 223 (1968)
2. D. Psaltis, F. Mok: American, 52 (November 1995)
3. V. Leyva, G.A. Rakuljic, B. O'Conner: Appl. Phys. Lett. **65**, 1079 (1994)
4. K. Buse: Appl. Phys. B **64**, 273 (1997)
5. K. Buse: J. Opt. Soc. Am. B **10**, 1266 (1993)
6. S. Ducharme: Opt. Lett. **16**, 1791 (1991)
7. V.L. Vinetskii, M.A. Itskovskii: Ferroelectrics **18**, 81 (1978)
8. K. Buse, K.H. Ringhofer: Appl. Phys. A **57**, 161 (1993)
9. K. Buse, R. Pankrath, E. Krätzig: Opt. Lett. **19**, 260 (1994)
10. W.W. Clark III, G.L. Wood, M.J. Miller, E.J. Sharp, G.J. Salamo, B. Monson, R.R. Neurgaonkar: Appl. Opt. **29**, 1249 (1990)
11. P.L. Ramazza, M. Zhao: Opt. Commun. **102**, 93 (1993)
12. M.P. Petrov, S.I. Stepanov, A.V. Khomenko: *Photorefractive Crystals in Coherent Optics* (Springer, Berlin, Heidelberg 1991)
13. K. Buse, U. van Stevendaal, R. Pankrath, E. Krätzig: J. Opt. Soc. Am. B **13**, 1461 (1996)
14. A.S. Bhalla, R.E. Newnham: Phys. Status Solidi A **58**, K19 (1980)
15. S. Ducharme, J. Feinberg, R.R. Neurgaonkar: IEEE J. Quantum Electron. **23**, 2116 (1987)
16. A.V. Mamaev, M. Saffman, A.A. Zozulya: Europhys. Lett. **35**, 25 (1996)